

# The least constrained supersymmetry with R-parity violation

Jinmian Li<sup>a,\*</sup> Tianjun Li<sup>b,c,†</sup> and Wenxing Zhang<sup>b,c‡</sup>

<sup>a</sup> *School of Physics, Korea Institute for Advanced Study, Seoul 02455, Korea*

<sup>b</sup> *CAS Key Laboratory of Theoretical Physics, Institute of Theoretical Physics, Chinese Academy of Sciences, Beijing 100190, China and*

<sup>c</sup> *School of Physical Sciences, University of Chinese Academy of Sciences, No. 19A Yuquan Road, Beijing 100049, China*

## Abstract

The strong constraints on the R-parity conserving supersymmetry (SUSY) from the LHC searches motivate us to consider the new models in which the low-scale SUSY is still allowed. We propose a kind of R-parity violating SUSY scenarios with a non-zero  $U_2^\xi D_2^c D_3^\xi$  operator. Three relevant LHC searches are recasted to test the status of this scenario in terms of four simplified models, with either light stop-Bino, stop-Higgsino, sbottom-Bino or sbottom-Higgsino. Some difficult scenarios for the LHC SUSY searches in these simplified models are identified. By extrapolate the current LHC searches to the future 14 TeV LHC with integrated luminosity of 300  $\text{fb}^{-1}$ , most of the difficult scenarios can be probed, except the sbottom-Bino simplified one. An improved search, which utilises the multiple b-jets as well as its kinematic features, is expected to probe the signature of this case.

Keywords:

---

<sup>\*</sup>jmli@kias.re.kr

<sup>†</sup>tli@itp.ac.cn

<sup>‡</sup>zhangwenxing@itp.ac.cn

## I. INTRODUCTION

As one of the most promising candidates for new physics beyond the Standard Model (SM), supersymmetry (SUSY) [1, 2] provides an elegant solution to the gauge hierarchy problem. In the Supersymmetric SMs (SSMs), the gauge coupling unification can be realized. In order to forbid the renormalizable superpotential terms which induce the fast proton decays, the  $Z_2$   $R$ -parity ( $R = (-1)^{(3B-L)+2S}$ ) is introduced, where  $B$ ,  $L$ , and  $S$  are baryon number, lepton number, and particle spin, respectively. Under the  $R$ -parity symmetry, all the SM particles are even while their superpartners are odd. Thus, the Lightest Supersymmetric Particle (LSP) will be stable. Especially, the neutralino LSP serves as the very promising weakly-interacting-massive-particle dark matter (DM) candidate, which can have the correct DM relic density as well [3].

However, the searches for  $R$ -parity conserving (RPC) SUSY signals at the LHC, which mainly rely on the large missing transverse energy (MET) in the final state, have given the strong constraints. The gluino/squark masses have been pushed to a couple of TeV scale [4, 5], challenging the naturalness problem [6, 7] and little hierarchy problem [8, 9] of the SUSY theories. On the other hand, the main goal for SUSY is to solve the gauge hierarchy problem, so  $R$ -parity is not mandatory. The  $R$ -parity violation (RPV) terms in the superpotential are [10]:

$$\mathcal{W} = \mu'_i L_i H_u + \lambda_{ijk} L_i L_j E_k^c + \lambda'_{ijk} L_i Q_j D_k^c + \lambda''_{ijk} U_i^c D_j^c D_k^c \quad (1.1)$$

where  $L_i$ ,  $E_i^c$ ,  $Q_i$ ,  $U_i^c$ ,  $D_i^c$  and  $H_u$  denote the left-handed lepton, right-handed lepton, left-handed doublet quarks, right-handed up-type quarks, right-handed down-type quarks and up-type higgs. The  $\lambda$  and  $\lambda''$  are antisymmetric in exchange of  $i \rightarrow j$  and  $j \rightarrow k$  respectively. In Eq. (1.1), the first three terms break the lepton number symmetry and the last term breaks the baryon number symmetry. Note that proton can still be stable as long as only the lepton number or baryon number symmetry is broken.

The RPV SUSY has been searched at the LHC [11, 12] in several different channels, with special attention paid to the gluino and top squark productions. The signature of pure hadronic multi-jet [13] in the final state has been searched to constrain the gluino pair production if  $\lambda''_{ijk}$ ,  $i \neq 3$  is non-zero. When  $\lambda''_{3jk} \neq 0$ , there could be top quarks from the gluino decay, the leptonic decay of which gives leptons + multi-jet final state [14–16]. Searches for the same final state are also constraining the  $L_i Q_j D_k^c$  operator. These operators will also lead to stop either decaying into two jets or decaying into a lepton and a jet, which has been searched in resonant di-jet pair [17] and lepton-jet pair [18]. Finally, if the RPV couplings are small such that the  $R$ -hadrons are stable at the scale of detector size, there are searches for long-lived  $R$ -hadrons [19]. From those searches, we can observe that the bounds obtained for those operators giving leptons in the final state are quite stringent, e.g. gluino being excluded up to  $\sim 2$  TeV, stop being excluded up to  $\sim 1$  TeV. As a result, these scenarios will be also in tension with the naturalness problem, same as for the RPC case. But the bounds with  $U_i^c D_j^c D_k^c$  operator are much weaker due to the large hadronic activity expected at the LHC [20–25]. There are plenty of studies that try to improve the sensitivity for RPV scenario with non-zero  $\lambda''_{ijk}$ , by using jet substructure analysis on either neutralino jet [26] or top squark jet [27, 28], and by multivariate analyses [29].

Among all possible  $\lambda''_{ijk}$ , the scenario with  $i = 3$  will give top quark in the final state from the on-shell/off-shell neutralino decay. The leptonic mode of which will be

stringently constrained. Moreover, terms with  $i, j, k = 1, 2$  are constrained [30] by the low energy experiments such as single nucleon decay channels and neutron-antineutron oscillation. In this paper, we will consider the least constrained scenario, i.e. RPV with only one non-zero  $\lambda''_{223}$ . This coupling is only constrained by the renormalisation group and its size is allowed to be as large as 1.25. In the experiment searches as well as some phenomenological studies, the RPV bounds on top/bottom squark are studied under the assumption that they are the LSP and 100% decay through the RPV operator. However, this might not be true in the SSMs inspired by a Grand Unified Theory (GUT) [31], where the lightest neutralino is the LSP. We will study the top/bottom squark bounds in the cases either there is Bino or Higgsino LSP. Then, the top squark can only decay into on-shell/off-shell top quark and a neutralino, which further decay through the RPV operator  $U_2^c D_2^c D_3^c$ , *i.e.*,  $csb$ . While the bottom squark decay is more complicated, beside the RPC decay of  $\tilde{b} \rightarrow b\tilde{\chi}^0/\tilde{b} \rightarrow t^*\tilde{\chi}^\pm$ , there is also direct RPV decay  $\tilde{b} \rightarrow cs$ .

This paper is organized as follows. In Sec. II, we introduce four simplified SUSY models with  $U_2^c D_2^c D_3^c$  R-parity violating operator. Their corresponding LHC signals will be discussed. In Sec. III, the current LHC sensitivities to those signals as well as their future prospects are studied. Our conclusions are given in Sec. IV. We also show the validation of our recasting of experimental searches in Appendices A- C.

## II. THE SIMPLIFIED MODELS AND SIGNALS

We consider the simplified RPV SUSY models with following assumptions:

- $\lambda''_{223}$  is the only non-vanishing RPV coupling.
- The only light colored particle is a right-handed dominant bottom squark or top squark, while all the others are too heavy to be produced at the LHC.
- Inspired from SUSY GUT as well as SUSY naturalness, we assume there is either an Bino ( $\tilde{B}$ ) or a Higgsino ( $\tilde{H}$ ) that has mass below the sbottom/stop, acting as the LSP.

As a result, we have four versions of simplified models:  $\tilde{t} - \tilde{B}$ ;  $\tilde{t} - \tilde{H}$ ;  $\tilde{b} - \tilde{B}$ ;  $\tilde{b} - \tilde{H}$ .

In the minimal SUSY framework, the tree-level mass matrix of the neutralino sector in the basis of  $(\tilde{B}, \tilde{W}^0, \tilde{H}_d^0, \tilde{H}_u^0)$  is

$$\mathcal{M} = \begin{pmatrix} M_1 & 0 & -m_Z \cos \beta \sin \theta_W & m_Z \sin \beta \sin \theta_W \\ 0 & M_2 & m_Z \cos \beta \cos \theta_W & -m_Z \sin \beta \cos \theta_W \\ -m_Z \cos \beta \sin \theta_W & m_Z \cos \beta \cos \theta_W & 0 & -\mu \\ m_Z \sin \beta \sin \theta_W & -m_Z \sin \beta \cos \theta_W & -\mu & 0 \end{pmatrix}, \quad (2.1)$$

where  $M_1$  and  $M_2$  are soft mass parameters for Bino and Wino,  $\mu$  is the bilinear Higgs mass in the superpotential, and  $\tan \beta$  is the ratio between the vacuum expectation values of  $H_u$  and  $H_d$ ,  $\theta_W$  is the weak mixing angle. The limit  $M_1 \ll M_2/\mu$  gives the Bino LSP in our simplified model. While the Higgsino LSP is more involved. In the limit  $\mu \ll M_1/M_2$ , there will be two mass eigenstates for neutralinos that have masses close to  $\mu$ . Both have similar amount of  $H_u$  and  $H_d$  component. Their mass difference is given

by

$$M_{\tilde{\chi}_2^0} - M_{\tilde{\chi}_1^0} = \frac{m_Z^2}{2} \left( \frac{\sin^2 \theta_W}{M_1} + \frac{\cos^2 \theta_W}{M_2} \right), \quad (2.2)$$

which is tiny in the decouple limit  $\mu \ll M_1/M_2$ . Moreover, the Higgsino has another component in the chargino sector. The chargino mass matrix can be written as

$$\mathcal{X} = \begin{pmatrix} M_2 & \sqrt{2}m_Z \cos \theta_W \sin \beta \\ \sqrt{2}m_Z \cos \theta_W \cos \beta & \mu \end{pmatrix}. \quad (2.3)$$

The mass difference between the charged Higgsino and the lighter neutral Higgsino is thus given by

$$M_{\tilde{\chi}_1^\pm} - M_{\tilde{\chi}_1^0} = \frac{m_Z^2}{2} \left[ \sin 2\beta \left( \frac{\sin^2 \theta_W}{M_1} - \frac{\cos^2 \theta_W}{M_2} \right) + \left( \frac{\sin^2 \theta_W}{M_1} + \frac{\cos^2 \theta_W}{M_2} \right) \right]. \quad (2.4)$$

It can be simplified further in the large  $\tan \beta$  limit:

$$M_{\tilde{\chi}_1^\pm} - M_{\tilde{\chi}_1^0} = \frac{m_Z^2}{2} \left( \frac{\sin^2 \theta_W}{M_1} + \frac{\cos^2 \theta_W}{M_2} \right). \quad (2.5)$$

To conclude, we will have two neutralinos and one chargino for the Higgsino LSP cases. All of those three particles have mass close to  $\mu$ . For specification and simplicity, we will take  $m_{\tilde{\chi}^\pm} = m_{\tilde{\chi}_2^0} + 1 = m_{\tilde{\chi}_1^0} + 1$  GeV throughout this work.

The dominant SUSY signal of these simplified models at the LHC are the sbottom/stop pair productions with their subsequent decays. Their productions are simply through the QCD couplings, thus with approximatively identical cross section for stop and sbottom. In Fig. 1, we plot the production cross section of sbottom at 8 TeV, 13 TeV and 14 TeV proton-proton collider.

The decays of stop/sbottom are more complicate. we will discuss each of the simplified models case by case.

- $\tilde{t} - \tilde{B}$ : The only allowed channel for the stop decay is  $\tilde{t} \rightarrow t^* \tilde{\chi}^0$ , with  $\tilde{\chi}^0 = \tilde{B}$  and top quark being either on-shell or off-shell depending on the mass difference between  $\tilde{t}$  and  $\tilde{\chi}^0$ , as shown in the left panel of Fig. 2.
- $\tilde{t} - \tilde{H}$ : Since there is also charged Higgsino lighter than the stop, beside the channel  $\tilde{t} \rightarrow t^* \tilde{\chi}_{1,2}^0$ , there is decay of  $\tilde{t} \rightarrow b \tilde{\chi}^\pm$  with subsequent decay  $\tilde{\chi}^\pm \rightarrow W^* \tilde{\chi}_1^0$ <sup>1</sup>, shown in the right panel of Fig. 2. When the stop is right-handed dominating, the decay width of each channel is given by

$$\Gamma(\tilde{t}_R \rightarrow t \tilde{H}_{1,2}^0) = \frac{1}{16\pi m_{\tilde{t}}^2} \left( \frac{Y_t}{\sqrt{2}} \right)^2 (m_{\tilde{t}}^2 - m_t^2 - m_{\tilde{H}_{1,2}^0}^2) \lambda^{1/2} (m_{\tilde{t}}^2, m_t^2, m_{\tilde{H}_{1,2}^0}^2), \quad (2.6)$$

$$\Gamma(\tilde{t}_R \rightarrow b \tilde{H}^\pm) = \frac{1}{16\pi m_{\tilde{t}}^2} (Y_t)^2 (m_{\tilde{t}}^2 - m_b^2 - m_{\tilde{H}^\pm}^2) \lambda^{1/2} (m_{\tilde{t}}^2, m_b^2, m_{\tilde{H}^\pm}^2), \quad (2.7)$$

---

<sup>1</sup> The direct RPV decays of chargino  $\tilde{\chi}^\pm \rightarrow tcs/ssb/ccb$  are assumed to be subdominant.

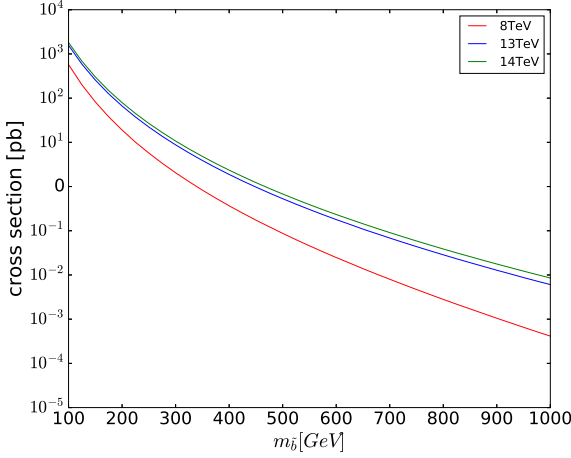


FIG. 1: Bottom squark production cross section at 8 TeV, 13 TeV and 14 TeV proton-proton collider.

with the two-body phase space function  $\lambda(x, y, z) = x^2 + y^2 + z^2 - 2(xy + xz + yz)$  and  $Y_t$  is the top quark Yukawa coupling. These two channels are comparable if they are kinematically allowed, while the later one is dominating when the mass difference between the stop and Higgsino is small ( $m_{\tilde{t}} < m_t + m_{\tilde{H}}$ ).

- $\tilde{b} - \tilde{B}$ : Firstly, the sbottom can decay through the RPC channel with decay width

$$\Gamma(\tilde{b}_R \rightarrow b\tilde{B}^0) = \frac{1}{16\pi m_{\tilde{b}}^2} \left( \frac{\sqrt{2}e}{3\cos\theta_W} \right)^2 (m_{\tilde{b}}^2 - m_b^2 - m_{\tilde{B}}^2) \lambda^{1/2}(m_{\tilde{b}}^2, m_b^2, m_{\tilde{B}}^2), \quad (2.8)$$

where  $Y_b$  is the bottom Yukawa coupling. In the mass limit  $m_{\tilde{b}} \gg m_b/m_{\tilde{B}}$ , the decay width can be estimated as  $\Gamma(\tilde{b} \rightarrow b\tilde{B}^0) \sim 0.013 \times \frac{m_{\tilde{b}}}{8\pi}$ . In contrast to the  $\tilde{t} - \tilde{B}$  simplified model, the sbottom can also decay directly through the RPV operator  $U_2^c D_2^c D_3^c$ . Its decay width can be written as

$$\Gamma(\tilde{b} \rightarrow \bar{s}\bar{c}) = \frac{m_{\tilde{b}}}{8\pi} |\lambda''_{223}|^2. \quad (2.9)$$

Thus, the decay width in Eqs. (2.8) and (2.9) will be around the same size if the  $\lambda''_{223} \sim \mathcal{O}(0.1)$ .

- $\tilde{b} - \tilde{H}$ : This case is similar with the  $\tilde{t} - \tilde{H}$  simplified model. The sbottom can decay either through  $\tilde{b} \rightarrow b\tilde{H}_{1,2}^0$  or  $\tilde{b} \rightarrow t\tilde{H}^\pm$ . Comparing to Eqs. (2.6) and (2.7), the decay widths of both channels are proportional to bottom quark Yukawa coupling instead of top quark Yukawa coupling, for the pure right-handed sbottom <sup>2</sup>.

<sup>2</sup> We note that the decay width of left-hand sbottom  $\Gamma(\tilde{b}_L \rightarrow t\tilde{H}^\pm) \propto Y_t^2$ . Because  $Y_t \gg Y_b$ , even small component of left-handed sbottom will lead to  $\Gamma(\tilde{b} \rightarrow t\tilde{H}^\pm) \gg \Gamma(\tilde{b} \rightarrow b\tilde{H}_{1,2}^0)$ , giving more top quarks

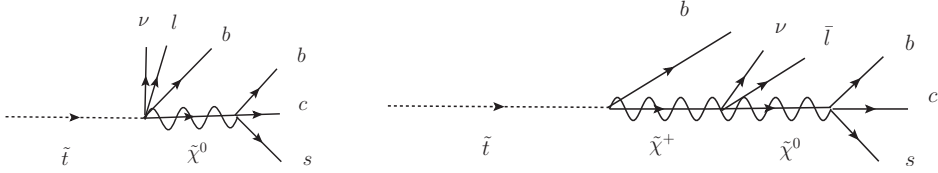


FIG. 2: Top squark decays channels in our simplified models.

In our setup, the neutralino will decay into three-body final states through an off-shell squark ( $\tilde{b}/\tilde{s}/\tilde{c}$ ). We should require that the decay length be within the detector. Otherwise, the neutralino will leave nothing inside the detector, behaving exactly the same as in RPC case. The RPV three body decay width of neutralino is [32]

$$\Gamma(\tilde{\chi}_1^0 \rightarrow bcs) = \frac{m_{\tilde{\chi}_1^0}^5}{1024\pi^3 m_{\tilde{q}}^4} |\lambda''_{223}|^2 C^2 \cdot I(m_{\tilde{q}}, m_{\tilde{\chi}_1^0}), \quad (2.10)$$

where we have assumed that all the quark masses are negligible, the phase space integral

$$I(m_{\tilde{q}}, m_{\tilde{\chi}_1^0}) = \int_0^1 \frac{12z^2(1-z)}{(1 - (1-z)\frac{m_{\tilde{\chi}_1^0}^2}{m_{\tilde{q}}^2})^2} \quad (2.11)$$

and  $C$  is coupling between the  $\tilde{\chi}_1^0 - q - \tilde{q}$ . For  $m_{\tilde{\chi}_1^0} \sim 100$  GeV,  $C \sim 0.1$  and  $m_{\tilde{q}} \gg m_{\tilde{\chi}_1^0}$ ,  $|\lambda''_{223}|/m_{\tilde{q}}^2 > 8.0 \times 10^{-9}$  is required, in order for neutralino to decay within  $\mathcal{O}(1)$  mm.

For the heavier neutralino  $\tilde{\chi}_2^0$  and the chargino  $\tilde{\chi}^\pm$  in the Higgsino LSP case, both particles are assumed to be dominated by the RPC decay, *i.e.*,  $\tilde{\chi}_2^0 \rightarrow h^*/Z^*\tilde{\chi}_1^0$  and  $\tilde{\chi}^\pm \rightarrow W^*\tilde{\chi}_1^0$ . Due to the compressed spectrum of Higgsino sector, the final states from the off-shell bosons ( $h^*, Z^*, W^*$ ) are too soft to be detected and only the  $\tilde{\chi}_1^0$  is visible. As a result, all of the three Higgsinos leave the same signal at the detector, that are three jets and one of them is  $b$ -tagged. In fact, if the RPV decays of  $\tilde{\chi}_2^0$  and  $\tilde{\chi}^\pm$  are important, *i.e.*, the  $\tilde{\chi}_2^0 \rightarrow bcs$  and  $\tilde{\chi}^\pm \rightarrow tcs/ssbccb$  are opening. The detector signals remain the same, except for the  $\tilde{\chi}^\pm \rightarrow tcs$  channel, which produces an extra top quark in the final state.

### III. TESTING WITH LHC SEARCHES

In this work, our signal events are generated by MG5\_aMC@NLO v2.6.0 [33], where PYTHIA8 [34], FASTJET-3.2.1 [35] and DELPHES-3.4.0 [36] have been used to implement parton showering, jet reconstruction and detector effects.

---

in the final state. Considering this, we will give sbottom a little mixing of left-handed part and focus on the  $\Gamma(\tilde{b} \rightarrow t\tilde{H}^\pm)$  case. Besides, there is direct RPV channel  $\tilde{b} \rightarrow sc$ , with its decay width given in Eq. (2.9) as well.

### A. Analysis and results under 13 TeV data

As discussed in the previous section, our signals include dijet resonance ( $\tilde{b} \rightarrow cs$ ), multi-jet ( $\tilde{t} \rightarrow b\tilde{\chi}^\pm/\tilde{b} \rightarrow b\tilde{\chi}^0$ ) and lepton + jets ( $\tilde{t} \rightarrow t\tilde{\chi}^0/\tilde{b} \rightarrow t\tilde{\chi}^\pm$ ). Even though most of our specific signals have not been searched at the LHC yet, there are some existing searches for the similar final states which could already constrain our signal processes. We will recast three relevant RPV SUSY searches from ATLAS: a lepton plus high jet multiplicity search [14], pair-produced resonances in four-jet final states [17] and multi-jet final states [37]. The validations of our recasting are provided in appendices.

To derive the bounds from recasting, a variable  $R^{ai} = N_{NP}^{ai}/N_{UL}^{ai}$  is defined in each signal region  $i$  of each analysis  $a$ , where  $N_{NP}^{ai}$  is the number of our signal events in the signal region  $i$  of analysis  $a$  obtained from our simulation and  $N_{UL}^{ai}$  is the observed 95% C.L. model independent upper limit provided in each experimental analysis. The maxima  $R^{\max} = \max_{a,i}\{R^{ai}\}$  is defined as the most sensitive one from all of the searches. This means a signal point is excluded by the current search if  $R^{\max} > 1$ .

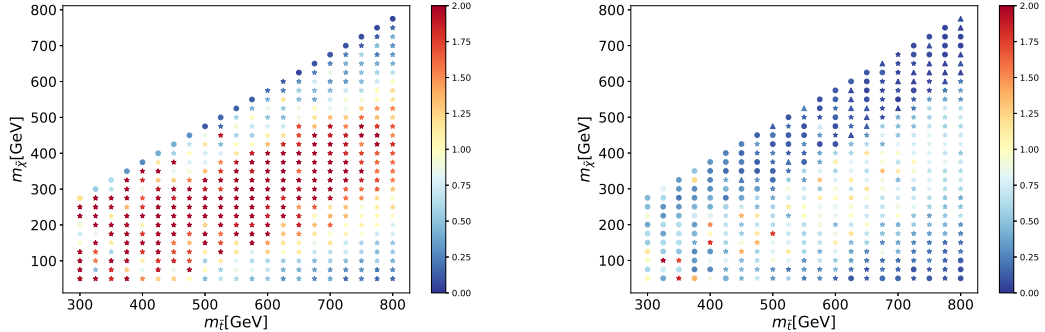


FIG. 3: Left panel: bounds on the  $\tilde{t} - \tilde{B}$  simplified model. Right panel: bounds on the  $\tilde{t} - \tilde{H}$  simplified model. The color bar shows the maximal  $R$  value obtained among all the experimental analyses. The most sensitive analysis at each grid is indicated by the point shapes. Points in the shapes of stellar, circular and triangle correspond to the analyses in Refs. [14], [17], and [37], respectively.

In Fig. 3, we plot the  $R^{\max}$  values in color on the  $m_{\tilde{t}}-m_{\tilde{\chi}^0}$  plane for  $\tilde{t} - \tilde{B}$  and  $\tilde{t} - \tilde{H}$  simplified model. The most sensitive search on each grid are indicated by the point shapes: stellar, circular and triangle correspond to the lepton plus high jet multiplicity analysis [14], pair-produced resonances in four-jet final state analysis [17] and multi-jet final state analysis [37], respectively.

In the  $\tilde{t} - \tilde{B}$  simplified model, because of the on-shell/off-shell top quark in the final state which could decay leptonically, the lepton plus jets search is the most sensitive one for most of the time. The constraint on this model is quite stringent, except for the regions with  $m_{\tilde{t}} \sim m_{\tilde{\chi}^0}$  or relatively light Bino. In the former region the lepton from top decay is too soft. While for too light Bino, the three jet from RPV  $\tilde{\chi}^0$  decay will be collimated, performing as a single jet in the detector. Thus, the jet multiplicity in the final state is reduced.

The bounds obtained in the  $\tilde{t} - \tilde{H}$  simplified model is much weaker, mainly because of the branching ratio suppression for each channel, *i.e.*,  $\tilde{t} \rightarrow t\tilde{\chi}^0$  and  $\tilde{t} \rightarrow b\tilde{\chi}^\pm$  produce the final states with and without detectable lepton. From the figure, we can see that still the lepton plus jets search is most sensitive one in most region. This means the current searches are only sensitive to the  $\tilde{t} \rightarrow t\tilde{\chi}^0$  while the  $\tilde{t} \rightarrow b\tilde{\chi}^\pm$  mode which produces an energetic  $b$ -jet is overlooked.

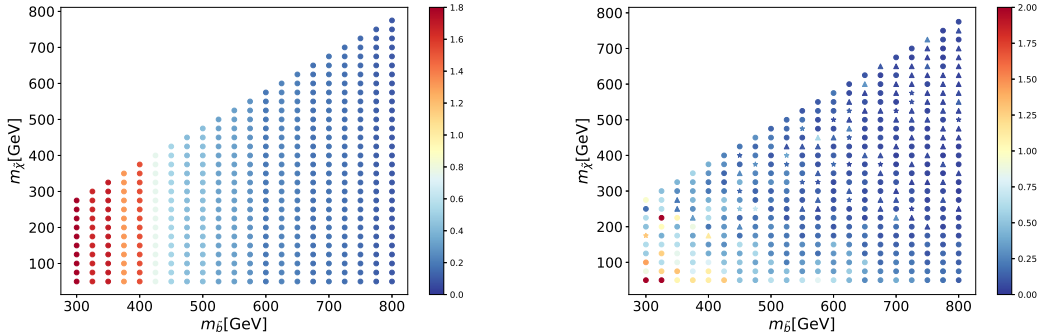


FIG. 4: Bounds on the  $\tilde{b} - \tilde{B}$  simplified model with  $\text{Br}(\tilde{b} \rightarrow cs) = 100\%$  (left) and  $\text{Br}(\tilde{b} \rightarrow b\tilde{\chi}^0) = 100\%$  (right). Point style same with Fig. 3.

For both the  $\tilde{b} - \tilde{B}$  and  $\tilde{b} - \tilde{H}$  simplified models, there is direct RPV sbottom decay  $\tilde{b} \rightarrow cs$ . At the LHC, there is a search [17] for stop pair which decay into  $sd$  or  $bs$  through non-zero  $\lambda''_{312}$  or  $\lambda''_{323}$  which coincide with our scenario when  $\text{Br}(\tilde{b} \rightarrow cs) = 100\%$ . The corresponding bounds are presented in the left panel of Fig. 4. Similar to the stop case, the sbottom with mass below  $\sim 425$  GeV has been excluded in this scenario.

In the  $\tilde{b} - \tilde{B}$  simplified model, beside the direct RPV decay, sbottom can decay into  $b\tilde{\chi}^0$  with subsequent RPV decay  $\tilde{\chi}^0 \rightarrow bcs$ . This channel is the most difficult channel respecting to current searches: 1) it does not produce any lepton in the final state; 2) for  $m_{\tilde{b}} \sim \mathcal{O}(100)$  GeV, the final state jets are typically too soft to pass the jet selections in the multi-jet search. As we can see from the right panel of Fig. 4, the LHC searches are only able to exclude the corner with both light sbottom and neutralino. In this region, the sbottom cross section is large and the decay final states of neutralino are collimated, reconstructed as a single jet. So that the signal here is appeared to be similar as the dijet resonance  $\tilde{b} \rightarrow jj$ . The four-jet resonance search [17] provides the most sensitive probing in most region. Especially, for very light neutralino  $m_{\tilde{\chi}} \sim 25$  GeV, sbottom is excluded up to 425 GeV in this model, which is close to the limit obtained in the  $\text{Br}(\tilde{b} \rightarrow cs) = 100\%$  scenario.

We have also performed the test on the scenario with  $\text{Br}(\tilde{b} \rightarrow cs) = \text{Br}(\tilde{b} \rightarrow b\tilde{\chi}^0) = 50\%$ . Because both channels are dominantly constrained by the same search, *i.e.*, dijet resonances search [17], we find the distributions of  $R^{\max}$  of this scenario is similar to the right panel of Fig. 4. Note that the rate of true dijet events is reduced to 25%.

Finally, for the  $\tilde{b} - \tilde{H}$  simplified model, if the direct RPV decay of sbottom is sub-dominating, its final states are similar with that of the  $\tilde{t} - \tilde{H}$  simplified model for pure right-handed sbottom and similar with that of  $\tilde{b} - \tilde{B}$  simplified model when there is small component of left-handed sbottom. Taking the later case as an example, the left-

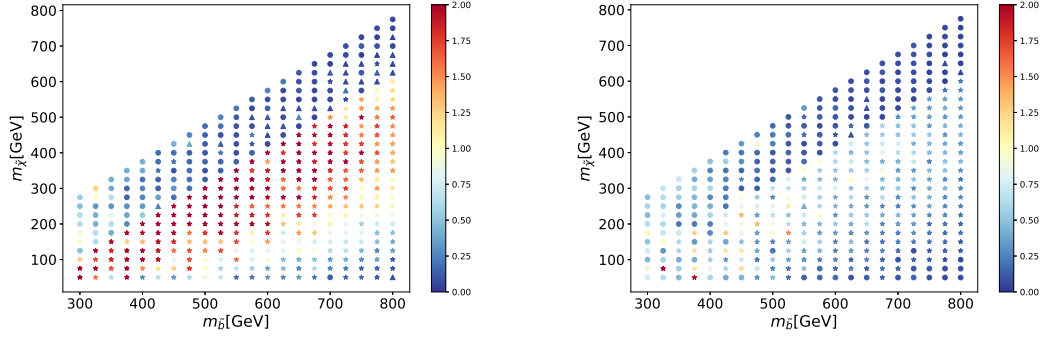


FIG. 5: Bounds on the  $\tilde{b} - \tilde{H}$  simplified model with  $\text{Br}(\tilde{b} \rightarrow cs) = 0\%$  (left) and  $\text{Br}(\tilde{b} \rightarrow cs) = 50\%$  (right). Point style same with Fig. 3.

handed sbottom mixing is taken to be 0.1 so that  $\tilde{b} \rightarrow t\tilde{H}^\pm$  dominates. The bounds are shown in the left panel of Fig. 5 which is similar to the left panel of Fig. 3. The lepton plus jets search is the most sensitive one, which exclude the region with  $m_{\tilde{b}} - 500 \text{ GeV} \lesssim m_{\tilde{H}} \lesssim m_{\tilde{b}} - m_t$ . The scenario with comparable branching ratios of detecting RPV decay  $\tilde{b} \rightarrow cs$  and subsequently decay  $\tilde{b} \rightarrow t\tilde{H}^\pm/b\tilde{H}^0$  will be more difficult to probe, due to the branching ratio suppression. The corresponding bound with  $\text{Br}(\tilde{b} \rightarrow cs) = 50\%$  are shown in the right panel of Fig 5. It shows that the current search can only exclude the region with  $m_{\tilde{b}} \sim [400, 500] \text{ GeV}$  and  $m_{\tilde{H}} \sim [100, 200] \text{ GeV}$ .

## B. Prospects with higher luminosity

From our above study, we have shown that the current searches are not yet able to excludes most of the parameter space, especially in the  $\tilde{t} - \tilde{H}$  simplified model, the  $\tilde{b} - \tilde{B}$  simplified model, and the  $\text{Br}(\tilde{b} \rightarrow cs) = 50\%$  scenario in the  $\tilde{b} - \tilde{H}$  simplified model. However, the  $R^{\text{max}}$  values on the most of the grids in those scenarios are already around  $\mathcal{O}(0.1)$ . It will be interesting to see the prospects of the sensitivity at higher luminosity LHC. In the following, we will simply extrapolate the exclusion limits at current stage to that of the future 14 TeV LHC with integrated luminosity of  $300 \text{ fb}^{-1}$ .

The following assumptions as adopted in Ref. [38] are made

- The definitions of signal regions are remained the same. Moreover, for both signal and background events, the selection efficiencies of each signal regions are almost kept the same from 13 TeV to 14 TeV.
- The statistical uncertainty of background is scaled by  $\sqrt{B}$ , where  $B$  is the total number of background events in the most sensitive signal region, *i.e.*, the one provides  $R^{\text{max}}$ .
- The systematic uncertainty is proportional to the  $B$ . Even through the systematic uncertainty of background is around 10%-20% in the current analysis, we expect some improvements in the future. So, we take the systematic uncertainty to be 5% in the extrapolation.

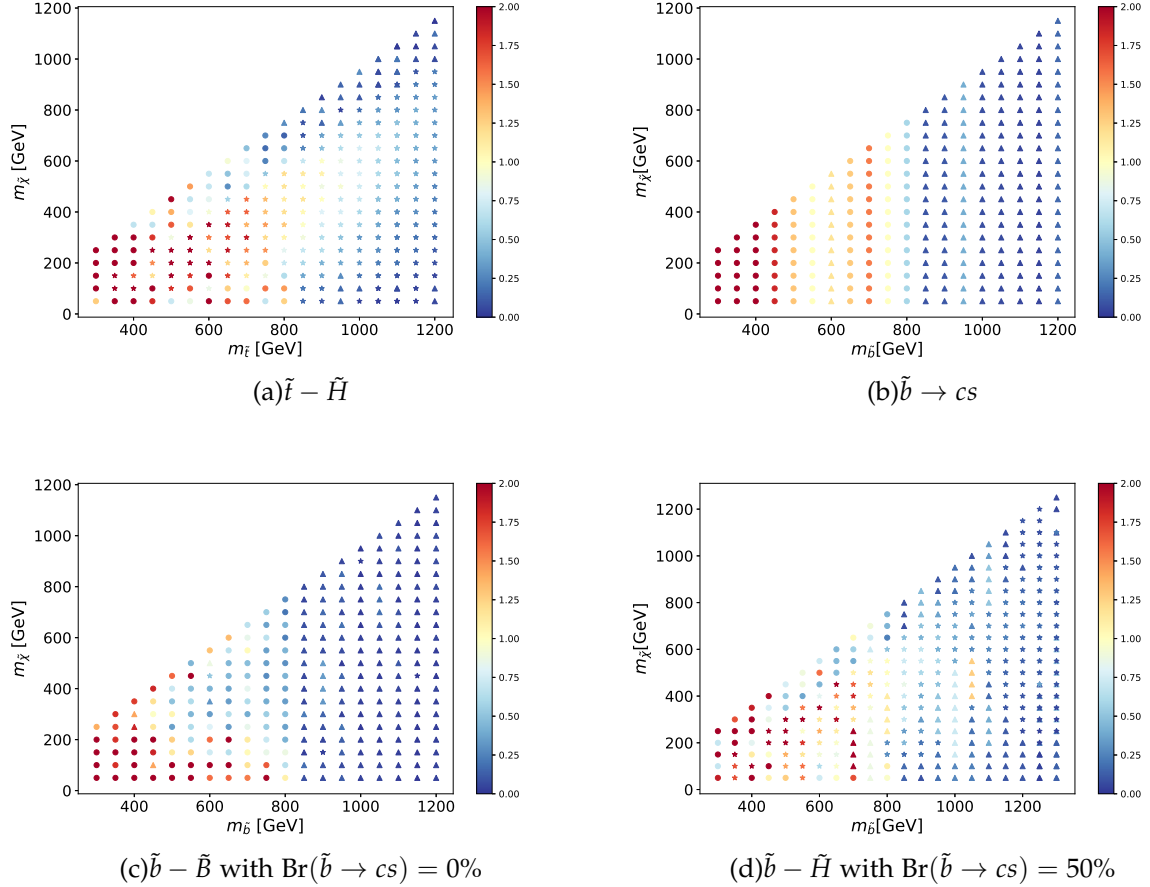


FIG. 6: The expected signal reaches at 14 TeV LHC with integrated luminosity of  $300 \text{ fb}^{-1}$ .

With these assumptions, the total number of signal and background events in a signal region is scaled by a factor of

$$F_{sig/bkg} = \frac{\mathcal{L}_0}{\mathcal{L}'} \times \frac{\sigma_{sig/bkg}(14 \text{ TeV})}{\sigma_{sig/bkg}(13 \text{ TeV})}, \quad (3.1)$$

where  $\sigma_{sig/bkg}(13/14 \text{ TeV})$  is the production cross sections of signal/background process at 13/14 TeV, and  $\mathcal{L}'/\mathcal{L}_0$  is the integrated luminosity of 13/14 TeV. Note only the dominant background process in each analysis is considered to estimate the scaling of background cross section. That is  $t\bar{t} + \text{jet}$  for the analysis in Ref. [14] and multi-jet for analyses in Refs. [17, 37] respectively. The scaled total number of background events ( $N_b$ ) together with the corresponding uncertainty ( $\sigma_b$ ) in each signal region can be used to calculate the model independent 95% C.L. new physics upper limit ( $N_{limit}$ ) in the signal region, which is defined as [39]

$$\frac{1}{\mathcal{N}} \int_0^{N_{limit}} \mathcal{L}(N_b|S, N_b, \sigma_b) P(S) dS = 0.95, \quad (3.2)$$

where  $\mathcal{N} = \int_0^{+\infty} \mathcal{L}(N_b|S, N_b, \sigma_b) P(S) dS$  is the normalization factor,  $P(S)$  is the prior probability of signal event number which is assumed to be uniform for all  $S$ . Taking into

account the uncertainties of background ( $\sigma_b$ ) and signal ( $\sigma_s$ ), the likelihood is defined as

$$\mathcal{L}(N_b|N_s, N_b, \sigma_b) = \frac{1}{2\pi\sigma_s\sigma_b} \int_{-5\sigma_s}^{5\sigma_s} d\delta_s \int_{-5\sigma_b}^{5\sigma_b} d\delta_b P(N_b; \mu) e^{\frac{\delta_b^2}{2\sigma_b^2}} e^{\frac{\delta_s^2}{2\sigma_s^2}}, \quad (3.3)$$

where  $\mu = N_s + N_b$  and  $P(N_b; \mu) = \frac{\mu^{N_b} e^{-\mu}}{N_b!}$  for  $N_b \leq 100$ ;  $P(N_b; \mu) = \frac{e^{\frac{(N_b - \mu)^2}{2\mu}}}{\sqrt{2\pi\mu}}$  for  $N_b > 100$ .

Finally, in each signal region, the ratio between the scaled number of signal events  $N_s$  and the  $N_{limit}$  is calculated. The maximal ratio  $R_{14}^{\max}$  among all signal regions is used to test a given model.

The extrapolated exclusion bounds for these difficult scenarios are shown in Fig. 6. Due to the increased signal event number and smaller systematics that we have assumed at 14 TeV with integrated luminosity of  $300 \text{ fb}^{-1}$ , the branching ratio suppression in the  $\tilde{t} - \tilde{H}$  simplified model becomes a less severe problem. There will be sufficient events with leptonic final states for the most of points with  $m_{\tilde{t}} \lesssim 1 \text{ TeV}$ . So the search for lepton plus high jet multiplicity excludes most of the region, except those with relatively degenerate spectrum so that lepton is too soft to be detected and those with heavy stop and light neutralino so that jet multiplicity is low. The upper-right panel of Fig. 6 shows the  $R_{14}^{\max}$  for the sbottom pair production with subsequent direct RPV decay  $\tilde{b} \rightarrow cs$ . The extrapolated dijet resonance search will push the bounds on sbottom mass to  $\sim 750 \text{ GeV}$ . In the higher mass region, where both the number and the energy of initial state radiated jets are increased, the multi-jet search becomes the most sensitive. As have been discussed above, the  $\tilde{b} - \tilde{B}$  is the most difficult model respecting to current searches. Moreover, including the direct RPV decay of sbottom does not change the current sensitivities in this model. In the lower-left panel of Fig. 6, we present the  $R_{14}^{\max}$  distribution in the scenario with  $\text{Br}(\tilde{b} \rightarrow cs) = 0\%$ . (We verified that the scenario with  $\text{Br}(\tilde{b} \rightarrow cs) = 50\%$  gives the similar result.) The future prospects for this model is still weak. The lower sbottom mass region can only be constrained by the dijet resonant search, which is not optimized for the signature of this model. And the multi-jet search only constrains the high sbottom mass region. As a consequence, sbottom as light as  $\sim 500 \text{ GeV}$  can not be fully excluded. The search sensitivity to the  $\tilde{b} - \tilde{H}$  model is much better, when the leptons in the final state can be energetic. For our choice of sbottom mixing, the signature of  $\text{Br}(\tilde{b} \rightarrow cs) = 0\%$  scenario of the  $\tilde{b} - \tilde{H}$  simplified model is similar to that of the  $\tilde{t} - \tilde{H}$  simplified model. Thus, it has similar bound as being presented in the upper-left panel of Fig. 6. In the lower-right panel, we present the bound for the  $\text{Br}(\tilde{b} \rightarrow cs) = 50\%$  scenario of this model, the constraint of which is weaker than that of  $\text{Br}(\tilde{b} \rightarrow cs) = 0\%$  scenario, simply because of the branching ratio suppression. The lepton plus jet search can exclude the sbottom mass in this scenario up to  $\sim 800 \text{ GeV}$ .

#### IV. CONCLUSION

In this paper, we proposed a RPV SUSY scenario that is least constrained by current LHC searches and low energy experiments, in which only the  $U_2^c D_2^c D_3^c$  operator is non-zero. Motivated by naturalness argument, four simplified models with relatively light stop/sbottom are considered, *i.e.*,  $\tilde{t} - \tilde{B}$ ,  $\tilde{t} - \tilde{H}$ ,  $\tilde{b} - \tilde{B}$ , and  $\tilde{b} - \tilde{H}$  models.

Those simplified model can lead to collider signatures of multiple jets, dijet resonance as well as leptons plus jets if any on-shell/off-shell top quarks are produced. By recasting the relevant LHC searches on our simplified model, we found some difficult scenarios for the current searches, where the stop/sbottom masses are barely constrained. They are  $\tilde{t} - \tilde{H}$  simplified model, the  $\tilde{b} - \tilde{B}$  simplified model, and the  $\text{Br}(\tilde{b} \rightarrow cs) = 50\%$  scenario in the  $\tilde{b} - \tilde{H}$  simplified model. Next, we extrapolated those existing searches to higher energy and luminosity LHC, *i.e.*, the 14 TeV 300  $\text{fb}^{-1}$  LHC. Under our assumptions in the extrapolation, the future prospects of the LHC sensitivities to those difficult scenarios are promising. Especially, the stop/sbottom up to 1 TeV can be probed in the  $\tilde{t} - \tilde{H}$  simplified model. However, since all current searches are not optimized on the signature of the  $\tilde{b} - \tilde{B}$  simplified model, the sbottom here is still very weakly constrained. The sbottom as light as  $\sim 500$  GeV can not be fully excluded. Note that the signature is featured by four b-jets and each two of them have the same origin. We expected that an improved search, which utilises these special features, can be sensitive to this model. As for the  $\text{Br}(\tilde{b} \rightarrow cs) = 50\%$  scenario in the  $\tilde{b} - \tilde{H}$  simplified model, the branching ratio suppression is substantial, and the sbottom with mass  $\sim 600$  GeV is still safe.

### Acknowledgements

We thank Chuang Li and Yizhou Fan for useful discussions. We especially thank Angelo Monteux for helping us to prove some of the results. In addition, we thank the Korea Institute for Advanced Study for providing computing resources (KIAS Center for Advanced Computation Linux Cluster System) for this work.

This research was supported in part by the Projects 11475238 and 11647601 supported by National Natural Science Foundation of China, and by Key Research Program of Frontier Science, CAS. The numerical results described in this paper have been obtained via the HPC Cluster of ITP-CAS.

### Appendix A: Search for a lepton plus multi-jet final states

Ref. [14] searches for final state with multi-jets and a lepton at 13 TeV 36  $\text{fb}^{-1}$  LHC. To validate our recasting, we take the second model in the paper, *i.e.*,  $pp \rightarrow \tilde{g}\tilde{g} \rightarrow \tilde{t}\tilde{t}(\rightarrow \bar{b}\bar{s})\tilde{t}\tilde{t}(\rightarrow \bar{b}\bar{s})$ .

We generate events for  $pp \rightarrow \tilde{g}\tilde{g}$  with MG5\_aMC@NLO v2.6.0 interfaced to PYTHIA8, which is used to decay  $\tilde{g}$ . In this step, the parton distribution function is provided by the NNPDF23LO. Then we do the detector simulation via DELPHES-3.4.0, with pile-up effect considered. The mass and detector parameters are  $M_{\tilde{t}} = 1.0$  TeV,  $M_{\tilde{g}} = 1.6$  TeV and the b-tag efficiency 78%.

In this analysis, only the total number of backgrounds and their uncertainties, the observation number are given (we will take the data in Tab. II of Ref. [14] as an example). We used the Eq. (3.2) to calculate the new physics upper limit for each signal region. The uncertainty of the observed event number  $\sigma_s$  is defined as  $\sigma_s = 0.1N_s$ . Our results are shown in Tab. I.

The final selection efficiencies of all signal region for our benchmark point have been given in the auxiliary Tab. II of Ref. [14], which refers to the row of "Exp" in our Tab. II.

		$\geq 10\text{jets}$		$\geq 11\text{jets}$		$\geq 12\text{jets}$	
Bkg		0b	$\geq 3b$	0b	$\geq 3b$	0b	$\geq 3b$
		$26 \pm 4$	$60 \pm 6$	$4.5 \pm 1.0$	$12.6 \pm 1.9$	$0.87 \pm 0.23$	$2.5 \pm 0.7$
Data		23	61	5	16	0	4
upper limit		12.7	24.5	7.0	13.2	3.0	7.1

TABLE I: The background and data are taken from the Tab. II of Ref. [14]. The last row gives the 95% C.L. new physics upper limit.

For comparison, the corresponding efficiencies from our simulation are provided in the last row of the same table, denoted as "Sim".

	$60\text{GeV}_{8\text{jets}}^{\geq 3\text{btags}}$	$60\text{GeV}_{9\text{jets}}^{\geq 3\text{btags}}$	$60\text{GeV}_{10\text{jets}}^{\geq 3\text{btags}}$	$80\text{GeV}_{8\text{jets}}^{\geq 3\text{btags}}$	$80\text{GeV}_{9\text{jets}}^{\geq 3\text{btags}}$	$80\text{GeV}_{10\text{jets}}^{\geq 3\text{btags}}$
Exp	4.8 %	2.6 %	1.0 %	2.9 %	1.2 %	0.4 %
Sim	5.7 %	2.8 %	1.2 %	3.0 %	1.3 %	0.37 %

TABLE II:

The final selections of some signal regions on our benchmark point: the numbers in the row of "Exp" are given in the auxiliary Tab. II of Ref. [14] and the results from our simulation are given in the row of "Sim".

## Appendix B: Search for dijet resonances

Paper [17] is a RPV search for pair-produced resonance in four-jet final states at  $\sqrt{s} = 13$  TeV, with luminosity  $36.7 \text{ fb}^{-1}$ . There are two kinds of *UDD* RPV vertices in this analysis, one is  $tsd$ , the other is  $tbs$ , we use the latter one to test, and set the top squark fully decays to  $bs$ . We generate  $pp \rightarrow \tilde{t}\tilde{t}$ , and choose stop mass 500 GeV. Signal samples are generated using MG5\_aMC@NLO v2.6.0 interfaced to PYTHIA8, with matching scale set about one quarter of dijet resonance mass, e.g.  $\sim 100$  GeV, then do detector simulation with DELPHES-3.4.0. The b tag efficiency is chosen as 77%, and the c-quark and light-quark mis-tagging efficiencies are 22.2% and 0.77%, respectively.

According to Eq. (3.2), we calculate the upper limits for all signal regions. The results are shown in Tab. III.

$m_{\tilde{t}}/\text{GeV}$	100	125	150	175	200	225	250	275	300	325
$N_{\text{limit}}$	199.38	462.98	704.55	524.46	774.34	353.98	443.62	357.81	216.86	202.32
$m_{\tilde{t}}/\text{GeV}$	350	375	400	425	450	475	500	525	550	575
$N_{\text{limit}}$	222.51	149.15	171.53	271.46	196.82	135.86	112.20	107.97	98.94	100.30
$m_{\tilde{t}}/\text{GeV}$	600	625	650	675	700	725	750	775	800	
$N_{\text{limit}}$	86.13	90.34	59.30	43.49	46.46	54.89	48.76	70.50	78.74	

TABLE III: New physics upper limits for all signal regions.

According to the Tab. I of Ref. [17], we present the corresponding numbers as well as efficiencies in Tab. IV, from which we could see that the recasting is successful.

	Total	Trigger	$\Delta R_{min}$	Inclusive selection	b-tagged selection
Exp	18400 (100%)	11900 (64.67%)	2470 (13.42%)	253 (1.38 %)	65 (0.35%)
Sim	19959 (100%)	13659 (68.44%)	2706 (13.56%)	211 (1.06%)	80 (0.40%)

TABLE IV: The analysis cutflows in the experimental paper (Exp) and from our simulation (Sim). Benchmark point with  $m_{\tilde{t}} = 500$  GeV is chosen in this study.

### Appendix C: Search for energetic multi-jet final state

In Ref. [37], the massive supersymmetric particles in multi-jet final states are searched. To validate our recasting, we consider the gluino direct decay model as adopted in this experimental analysis.

We generate  $pp \rightarrow \tilde{g}\tilde{g}$  with MG5\_aMC@NLO v2.6.0, then  $\tilde{g}$  fully decays to  $UDD$  quarks in PYTHIA8, where the mass of  $\tilde{g}$  is set to 1.1 TeV. Upper limit can be calculated using Eq. (3.2) as before, the results are given in Tab. V. The cuts flow of the analysis on the benchmark points have been provided in the Tab. 4 of Ref. [37]. For comparison, we present both the experimental result (Exp) and our simulated result (Sim) in Tab. VI.

Signal Region	4jSRb1	4jSR	5jSRb1	5jSR
Bkg	$61 \pm 10$	$151 \pm 15$	$18.2 \pm 4.2$	$51.4 \pm 7.7$
Obs	46	122	30	64
Upper Limit	26.05	46.03	29.6	43.51

TABLE V: The number of background events and their uncertainties as well as the observed event numbers in signal regions are provided in the Tab. 2 of Ref. [37]. In the last row, we calculate the new physics upper limit for each signal region.

	Trigger	$p_T^{lead} > 440$ GeV	$n_{jet} \geq 4$	$M_J^\Sigma > 0.8$ TeV	$ \Delta\eta_{12}  < 1.4$	$b - tag$
Exp	2401	2236(93.13%)	1159(48.27%)	63.3(2.63%)	56.6(2.36%)	43.3(1.80%)
Sim	2401	2107(87.76%)	1280(53.31%)	87.34(3.64%)	45.94(1.91%)	39.22(1.63%)

TABLE VI: Cut flow of the gluino direct decay model with  $m_{\tilde{g}} = 1100$  GeV in the experimental analysis (Exp) and from our simulation (Sim).

---

[1] H. P. Nilles, *Supersymmetry, Supergravity and Particle Physics*, *Phys. Rept.* **110** (1984) 1–162.  
[2] H. E. Haber and G. L. Kane, *The Search for Supersymmetry: Probing Physics Beyond the Standard Model*, *Phys. Rept.* **117** (1985) 75–263.

- [3] G. Jungman, M. Kamionkowski, and K. Griest, *Supersymmetric dark matter*, *Phys. Rept.* **267** (1996) 195–373, [[hep-ph/9506380](#)].
- [4] **ATLAS** Collaboration, M. Aaboud et al., *Search for squarks and gluinos in final states with jets and missing transverse momentum using 36  $fb^{-1}$  of  $\sqrt{s}=13$  TeV  $pp$  collision data with the ATLAS detector*, [arXiv:1712.02332](#).
- [5] **CMS** Collaboration, A. M. Sirunyan et al., *Search for natural and split supersymmetry in proton-proton collisions at  $\sqrt{s} = 13$  TeV in final states with jets and missing transverse momentum*, [arXiv:1802.02110](#).
- [6] L. J. Hall, D. Pinner, and J. T. Ruderman, *A Natural SUSY Higgs Near 126 GeV*, *JHEP* **04** (2012) 131, [[arXiv:1112.2703](#)].
- [7] M. Papucci, J. T. Ruderman, and A. Weiler, *Natural SUSY Endures*, *JHEP* **09** (2012) 035, [[arXiv:1110.6926](#)].
- [8] M. Bastero-Gil, C. Hugonie, S. F. King, D. P. Roy, and S. Vempati, *Does LEP prefer the NMSSM?*, *Phys. Lett.* **B489** (2000) 359–366, [[hep-ph/0006198](#)].
- [9] F. Bazzocchi and M. Fabbrichesi, *Little hierarchy problem for new physics just beyond the LHC*, *Phys. Rev.* **D87** (2013), no. 3 036001, [[arXiv:1212.5065](#)].
- [10] L. J. Hall and M. Suzuki, *Explicit R-Parity Breaking in Supersymmetric Models*, *Nucl. Phys.* **B231** (1984) 419–444.
- [11] A. Redelbach, *Searches for Prompt R-Parity-Violating Supersymmetry at the LHC*, *Adv. High Energy Phys.* **2015** (2015) 982167, [[arXiv:1512.05956](#)].
- [12] D. Dercks, H. Dreiner, M. E. Krauss, T. Opferkuch, and A. Reinert, *R-Parity Violation at the LHC*, *Eur. Phys. J.* **C77** (2017), no. 12 856, [[arXiv:1706.09418](#)].
- [13] **ATLAS** Collaboration, M. Aaboud et al., *Search for R-parity-violating supersymmetric particles in multi-jet final states produced in  $p$ - $p$  collisions at  $\sqrt{s} = 13$  TeV using the ATLAS detector at the LHC*, [arXiv:1804.03568](#).
- [14] **ATLAS** Collaboration, M. Aaboud et al., *Search for new phenomena in a lepton plus high jet multiplicity final state with the ATLAS experiment using  $\sqrt{s} = 13$  TeV proton-proton collision data*, *JHEP* **09** (2017) 088, [[arXiv:1704.08493](#)].
- [15] **CMS** Collaboration, A. M. Sirunyan et al., *Search for R-parity violating supersymmetry in  $pp$  collisions at  $\sqrt{s} = 13$  TeV using  $b$  jets in a final state with a single lepton, many jets, and high sum of large-radius jet masses*, *Submitted to: Phys. Lett. B* (2017) [[arXiv:1712.08920](#)].
- [16] **ATLAS** Collaboration, M. Aaboud et al., *Search for supersymmetry in final states with two same-sign or three leptons and jets using 36  $fb^{-1}$  of  $\sqrt{s} = 13$  TeV  $pp$  collision data with the ATLAS detector*, *JHEP* **09** (2017) 084, [[arXiv:1706.03731](#)].
- [17] **ATLAS** Collaboration, M. Aaboud et al., *A search for pair-produced resonances in four-jet final states at  $\sqrt{s} = 13$  TeV with the ATLAS detector*, *Eur. Phys. J.* **C78** (2018), no. 3 250, [[arXiv:1710.07171](#)].
- [18] **ATLAS** Collaboration, M. Aaboud et al., *Search for B-L R -parity-violating top squarks in  $\sqrt{s} = 13$  TeV  $pp$  collisions with the ATLAS experiment*, *Phys. Rev.* **D97** (2018), no. 3 032003, [[arXiv:1710.05544](#)].
- [19] **ATLAS** Collaboration, T. A. collaboration, *Reinterpretation of searches for supersymmetry in models with variable R-parity-violating coupling strength and long-lived R-hadrons*, .
- [20] B. C. Allanach and B. Gripaios, *Hide and Seek With Natural Supersymmetry at the LHC*, *JHEP* **05** (2012) 062, [[arXiv:1202.6616](#)].
- [21] G. Durieux and C. Smith, *The same-sign top signature of R-parity violation*, *JHEP* **10** (2013) 068, [[arXiv:1307.1355](#)].

[22] B. Bhattacherjee, J. L. Evans, M. Ibe, S. Matsumoto, and T. T. Yanagida, *Natural supersymmetry's last hope: R-parity violation via UDD operators*, *Phys. Rev.* **D87** (2013), no. 11 115002, [[arXiv:1301.2336](#)].

[23] S. Diglio, L. Feligioni, and G. Moultaka, *Stashing the stops in multijet events at the LHC*, *Phys. Rev.* **D96** (2017), no. 5 055032, [[arXiv:1611.05850](#)].

[24] M. R. Buckley, D. Feld, S. Macaluso, A. Monteux, and D. Shih, *Cornering Natural SUSY at LHC Run II and Beyond*, *JHEP* **08** (2017) 115, [[arXiv:1610.08059](#)].

[25] J. A. Evans and D. McKeen, *The Light Gluino Gap*, [arXiv:1803.01880](#).

[26] J. M. Butterworth, J. R. Ellis, A. R. Raklev, and G. P. Salam, *Discovering baryon-number violating neutralino decays at the LHC*, *Phys. Rev. Lett.* **103** (2009) 241803, [[arXiv:0906.0728](#)].

[27] Y. Bai, A. Katz, and B. Tweedie, *Pulling Out All the Stops: Searching for RPV SUSY with Stop-Jets*, *JHEP* **01** (2014) 040, [[arXiv:1309.6631](#)].

[28] B. Bhattacherjee and A. Chakraborty, *Study of the baryonic R-parity violating MSSM using the jet substructure technique at the 14 TeV LHC*, *Phys. Rev.* **D89** (2014), no. 11 115016, [[arXiv:1311.5785](#)].

[29] D. Bardhan, A. Chakraborty, D. Choudhury, D. K. Ghosh, and M. Maity, *Search for bottom squarks in the baryon-number violating MSSM*, *Phys. Rev.* **D96** (2017), no. 3 035024, [[arXiv:1611.03846](#)].

[30] R. Barbier et al., *R-parity violating supersymmetry*, *Phys. Rept.* **420** (2005) 1–202, [[hep-ph/0406039](#)].

[31] K. Kowalska, L. Roszkowski, E. M. Sessolo, and A. J. Williams, *GUT-inspired SUSY and the muon  $g - 2$  anomaly: prospects for LHC 14 TeV*, *JHEP* **06** (2015) 020, [[arXiv:1503.08219](#)].

[32] A. Monteux, *New signatures and limits on R-parity violation from resonant squark production*, *JHEP* **03** (2016) 216, [[arXiv:1601.03737](#)].

[33] J. Alwall, R. Frederix, S. Frixione, V. Hirschi, F. Maltoni, O. Mattelaer, H. S. Shao, T. Stelzer, P. Torrielli, and M. Zaro, *The automated computation of tree-level and next-to-leading order differential cross sections, and their matching to parton shower simulations*, *JHEP* **07** (2014) 079, [[arXiv:1405.0301](#)].

[34] T. Sjstrand, S. Ask, J. R. Christiansen, R. Corke, N. Desai, P. Ilten, S. Mrenna, S. Prestel, C. O. Rasmussen, and P. Z. Skands, *An Introduction to PYTHIA 8.2*, *Comput. Phys. Commun.* **191** (2015) 159–177, [[arXiv:1410.3012](#)].

[35] M. Cacciari, G. P. Salam, and G. Soyez, *FastJet User Manual*, *Eur. Phys. J.* **C72** (2012) 1896, [[arXiv:1111.6097](#)].

[36] **DELPHES 3** Collaboration, J. de Favereau, C. Delaere, P. Demin, A. Giammanco, V. Lematre, A. Mertens, and M. Selvaggi, *DELPHES 3, A modular framework for fast simulation of a generic collider experiment*, *JHEP* **02** (2014) 057, [[arXiv:1307.6346](#)].

[37] **ATLAS Collaboration** Collaboration, *Search for massive supersymmetric particles in multi-jet final states produced in  $pp$  collisions at  $\sqrt{s} = 13$  TeV using the ATLAS detector at the LHC*, *Tech. Rep. ATLAS-CONF-2016-057*, CERN, Geneva, Aug, 2016.

[38] **CMS Collaboration**, *Projected Performance of an Upgraded CMS Detector at the LHC and HL-LHC: Contribution to the Snowmass Process*, in *Proceedings, 2013 Community Summer Study on the Future of U.S. Particle Physics: Snowmass on the Mississippi (CSS2013): Minneapolis, MN, USA, July 29-August 6, 2013*, 2013. [arXiv:1307.7135](#).

[39] J. Guo, Z. Kang, J. Li, T. Li, and Y. Liu, *Simplified Supersymmetry with Sneutrino LSP at 8 TeV LHC*, *JHEP* **10** (2014) 164, [[arXiv:1312.2821](#)].